Dalton Transactions

ROYAL SOCIETY OF CHEMISTRY

PAPER

View Article Online
View Journal

Published on 02 November 2020. Downloaded by Carleton University on 11/21/2020 11:15:23 PM.

Check for updates

Cite this: DOI: 10.1039/d0dt02266g

# Synthesis of a series of novel In(III) 2,6-diacetylpyridine bis(thiosemicarbazide) complexes: structure, anticancer function and mechanism†

Shanhe Li,‡[a] Muhammad Hamid Khan,‡[a] Xiaojun Wang,‡[a] Meiling Cai,[a] Juzheng Zhang,[a] Ming Jiang,[a] Zhenlei Zhang,[a] Xiao-an Wen,[b] Hong Liang[a] and Feng Yang*[a]

The anticancer function and anticancer mechanism of indium (In) complexes still remain mysterious to date. Furthermore, it is greatly challenging to design a multi-functional metal agent that not only kills cancer cells but also inhibits their invasion and metastasis. Thus, to develop novel next-generation anticancer metal agents, we designed and synthesized a series of novel In(III) 2,6-diacetylpyridine bis(thiosemicarbazide) complexes (**C1–C4**) for the first time and then investigated their structure–activity relationships with human urinary bladder cancer (T-24) cells. In particular, **C4** not only showed higher cytotoxicity to cancer cells and less toxicity toward normal cells relative to cisplatin but also inhibited cell invasion and metastasis of T-24 cells. Interestingly, **C4** acted against T-24 cells exhibiting multiple mechanisms: (1) arresting the S-phase of cell cycle *via* regulation of cytokine kinases, (2) activating the mitochondrial-mediated apoptosis, endoplasmic reticulum-stress-mediated cell death, PERK and c-Jun N-terminal kinase 1 (JNK) cell signaling pathways, and (3) inhibiting the expression of telomerase *via* the regulation of c-myc and h-TERT proteins. Our results suggested that **C4** may be developed as a potential multi-functional and multi-targeting anticancer candidate.

Received 26th June 2020,
Accepted 29th October 2020

DOI: 10.1039/d0dt02266g

rsc.li/dalton

## 1 Introduction

Cancer has become one of the most serious diseases which pose a great threat to human health around the world. A number of new cancer diagnoses have been introduced, but the mortality rate in developed and developing countries is increasing.[1–3] About half of all the patients who receive anticancer chemotherapy are treated with cisplatin and its derivatives.[4,5] However, increased drug effluence, drug inactivation, variations in the drug target, and processing of drug-induced damage limited anticancer applications of platinum-based anticancer drugs.[6] This has encouraged researchers to employ different approaches in the development of new metal-based anticancer agents with different mechanisms of action.[7]

Recently, novel N-heterocyclic metal complexes showed potent cytotoxicity against numerous cancer cells. These complexes can make stable coordination bonds with numerous metal ions that could be more stable under physiological conditions and increase their target ability to cancer cells.[8–10] On the other hand, drugs that act against multiple targets of cancer cells can enhance therapeutic efficacy and lower their resistance relative to the single target-based therapy.[11–13]

Thiosemicarbazones that have extensive pharmacological flexibility and their application as antitumor, antiviral and antimicrobial agents have been widely studied.[14] Thiosemicarbazones, particularly N-heterocyclic thiosemicarbazides, have low π-electron density at the side chain and the ring N-atom has an electron-pair donor to transition metals to form coordination compounds.[15–18] Numerous studies have revealed that the coordination of thiosemicarbazones to metal ions increased the activity of the overall complex, enhanced the efficacy and overcame the deficiency of organic parent compounds.[19,20]

In general, "In" donates three outermost electrons to become the In(III) oxidation state. It could form stable In(III) complexes with ligands under physiological conditions and showed remarkable biological applications.[21,22] Owing to the advantages of the In complex, it may be a promising alterna-

[a]State Key Laboratory for the Chemistry and Molecular Engineering of Medicinal Resources, Ministry of Science and Technology of China, Guangxi Normal University, Guilin, Guangxi, China. E-mail: fyang@mailbox.gxnu.edu.cn; Fax: +86-773-584-8836; Tel: +86-773-584-8836
[b]Jiangsu Key Laboratory of Drug Discovery for Metabolic Disease, China Pharmaceutical University, Nanjing, Jiangsu, China

†Electronic supplementary information (ESI) available. CCDC 1961543, 1961545, 1961546 and 1961553. For ESI and crystallographic data in CIF or other electronic format see DOI: 10.1039/d0dt02266g

‡These authors contributed equally to this article.

Published on 02 November 2020. Downloaded by Carleton University on 11/21/2020 11:15:23 PM.

tive of Pt agents. However, only a few studies of In compounds have been reported to date.[23,24] Their anticancer functions and mechanisms still remain mysterious.

To develop novel next-generation anticancer metal agents, we focused on designing and synthesizing a series of In(III) 2,6-diacetylpyridine bis(thiosemicarbazide) complexes for the first time (Scheme S1†). In(III) complexes were modified at the N-4 position of the ligands and thoroughly analyzed by IR spectroscopy, mass spectroscopy, and $^1$H NMR spectroscopy and their multifunctional mechanisms were investigated by biological experiments. Subsequently, we not only investigated the structure–activity relationships of In complexes to human urinary bladder cancer (T-24) cells and their metastasis inhibition activity but also confirmed their multi-targeting mechanisms, including the activation of mitochondrial-mediated apoptosis, MAPK-mediated apoptosis, endoplasmic reticulum stress-mediated cell damage, and inhibition of telomerase activity.

# 2 Results

## 2.1 Design and structure of four In(III) complexes

N-Heterocyclic thiosemicarbazones are an established important class of N, S-donor ligands and studied for a considerable period of time because of their variable donor properties, structural diversity and biological applications.[25–27] N-Donor coordinated to metals enhances the anticancer activities of thiosemicarbazide ligands, particularly affecting multiple proteins related to cancer and inhibiting tumor growth *via* multiple mechanisms.[28] Specifically, 2,6-diacetylpyridine thiosemicarbazide and their N-4 position modified derivatives were used to design four novel In(III) complexes, namely, **C1**, **C2**, **C3** and **C4**. **C1–C4** were synthesized by a stirring protocol and crystallized by an evaporation method. The structures of **C1–C4** were identified by X-ray crystallography and solved by the Olex-2 application (Table 1) (Fig. 1).

**C1** is crystallized in the monoclinic space group $p2_1/n$ with one In(III) per complex. The In atoms of the dimer are hepta-coordinated, binding to three N-atoms and two S-atoms of the ligands and two terminal chlorine atoms of the complex. The central In atom of each of the ligand is surrounded by coordination polyhedra, which could be described as having pentagonal bipyramid geometry. The metal displacements of In1–Cl2, In1–Cl1, In1–S2, In1–S1, In1–N5, In1–N3, and In1–N4 are ranging from 2.328 Å to 2.6296 Å. The distinct In(III) dimer of the complex having bond angles of Cl2–In1–S2, Cl2–In1–S1, Cl1–In1–Cl2, Cl1–In1–S2, Cl1–In1–S1, S1–In1–S2, N5–In1–Cl2, N5–In1–Cl1, N5–In1–S2, N5–In1–S1, N3–In1–Cl2, N3–In1–Cl1, N3–In1–S2, N3–In1–S1, N3–In1–N5, N3–In1–N4, N4–In1–Cl2, N4–In1–Cl1, N4–In1–S2, N4–In1–S1, and N4–In1–N5 are ranging from 65.96° to 170.87°.

The structures of **C2–C4** were also characterized by single-crystal X-ray diffraction analysis and are similar to that of **C1** (Fig. 1). All relative crystal data are compiled in Tables S1 and S2.†

## 2.2 Stability of the In(III) complex under physiological conditions

The In(III) complexes were analyzed by UV-vis spectroscopy and investigated for their resistance to degradation in phosphate buffer (PBS) over time. **C1–C4** were dissolved in DMSO, and then diluted with PBS. The amount of DMSO in **C1–C4** solution is lower than 1%. Their UV-visible spectra were recorded at different times (0–48 h). As shown in Fig. S1,† no apparent red or blue shift in the absorption peaks of each group was shown, and no new absorption peak appeared. These results indicated that the structure of the In(III) complexes was stable and was not degradable in the solution for 48 h.

**Table 1** Crystal data of four In(III) complexes

| Identification code | C1 | C2 | C3 | C4 |
|---|---|---|---|---|
| Empirical formula | $C_{11}H_{13}Cl_2InN_7S_2$ | $C_{14}H_{22}Cl_2InN_7OS_2$ | $C_{46}H_{42}Cl_2In_2N_{14}S_4$ | $C_{16}H_{26}Cl_2InN_7OS_2$ |
| Formula weight | 494.13 | 554.22 | 1219.71 | 582.28 |
| Temperature/K | 296.15 | 296(2) | 296.15 | 293.15 |
| Crystal system | monoclinic | monoclinic | triclinic | monoclinic |
| Space group | $P2_1/n$ | $P2_1/c$ | $P\bar{1}$ | $C2/c$ |
| $a$/Å | 8.4977(13) | 10.820(7) | 8.5777(6) | 9.7761(3) |
| $b$/Å | 13.297(2) | 13.440(8) | 11.3038(8) | 14.2179(6) |
| $c$/Å | 15.646(2) | 15.215(9) | 13.9701(10) | 16.7170(11) |
| $\alpha$/° | 90.00 | 90.00 | 94.0320(10) | 90.00 |
| $\beta$/° | 103.015(2) | 100.058(8) | 102.8920(10) | 98.698(5) |
| $\gamma$/° | 90.00 | 90.00 | 106.2790(10) | 90.00 |
| Volume/Å$^3$ | 1722.4(5) | 2179(2) | 1254.63(15) | 2296.9(2) |
| $Z$ | 4 | 4 | 1 | 4 |
| $\rho_{calc}$ (g cm$^{-3}$) | 1.905 | 1.690 | 1.614 | 1.684 |
| $\mu$/mm$^{-1}$ | 1.933 | 1.541 | 1.241 | 1.466 |
| $F$(000) | 976.0 | 1112.0 | 612.0 | 1176.0 |
| Data/restraints/parameter | 3539/0/212 | 3821/2/249 | 5098/2/309 | 2683/112/145 |
| Goodness-of-fit on $F^2$ | 1.049 | 1.035 | 1.035 | 1.171 |
| Final $R$ indexes $[I \geq 2\sigma(I)]$ | $R_1$ = 0.0225, w$R_2$ = 0.0515 | $R_1$ = 0.0428, w$R_2$ = 0.1114 | $R_1$ = 0.0235, w$R_2$ = 0.0557 | $R_1$ = 0.0485, w$R_2$ = 0.0966 |
| Largest diff. peak/hole (e Å$^{-3}$) | 0.46/−0.62 | 1.05/−0.59 | 0.46/−0.26 | 0.89/−0.78 |
| CCDC | 1961553 | 1961543 | 1961545 | 1961546 |


This journal is © The Royal Society of Chemistry 2020

Published on 02 November 2020. Downloaded by Carleton University on 11/21/2020 11:15:23 PM.

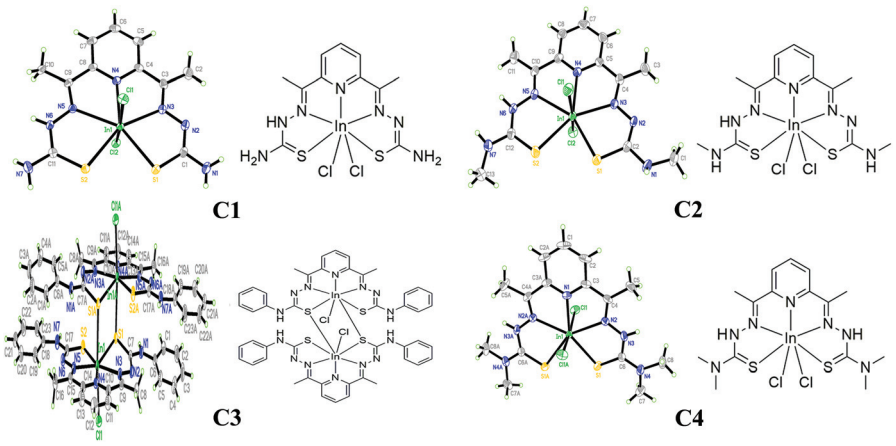


Fig. 1 X-ray crystallographic structures of In(III) complexes (**C1–C4**).

### 2.3 Structure–cellular uptake relationships of In(III) complexes

To conduct the cellular uptake study, we selected T24 cells. Inductively coupled plasma (ICP)-MS was used to measure the total intracellular indium and platinum content in T24 cells. We observed that In(III) complexes absorbed by T-24 cells were structure-dependent. As shown in Fig. S2,† the total intracellular contents of In and Pt ions in cells treated with **C1–C4** and cisplatin were measured with 1.02 nmol, 1.40 nmol, 1.69 nmol, 3.09 nmol, and 0.548 nmol, which were 13%, 18%, 21.8%, 39.8%, and 7.05% of the total intracellular In and Pt ions respectively. In the cytoplasm of T-24 cells, the concentrations of In and Pt ions in **C1–C4** and cisplatin-treated cells were found to be 58% (0.59 nmol), 59% (0.82 nmol), 61% (1.03 nmol), 60% (1.85 nmol), and 57% (0.31 nmol) of the total intracellular In and Pt ions, respectively. Similarly, the concentration of "In" in **C1–C4** treated cells and "Pt" in cisplatin-treated cells in the mitochondria of T-24 cells was found to be 24% (0.244 nmol), 19% (0.33 nmol), 22% (0.40 nmol), and 23% (0.74 nmol) and 20% (0.11 nmol), respectively, while the concentration of "In" in **C1–C4** treated cells and "Pt" in cisplatin-treated cells in the nucleus of T-24 cells was found to be 18% (18 nmol), 22% (0.31 nmol), 19% (0.32 nmol), and 17% (0.52 nmol) and 23% (0.126 nmol), respectively. These results suggested that the intracellular absorption of metals is structure-dependent. The modifications of the N4-position of the thiosemicarbazide ligands differentiate the efficacy of the In complexes. The presence of "In" measured in the mitochondria was higher than nucleus, suggesting the activation of mitochondrial-mediated apoptosis in tumor cells, which was further supported by the cytometric and western blot results.

### 2.4 Multi-functional anticancer In(III) complexes

**2.4.1 Structure–activity relationships of In(III) complexes.** The cytotoxicity of four N4-modified thiosemicarbazide ligands (**L1–L4**), four In(III) thiosemicarbazone complexes (**C1–C4**) and cisplatin was determined separately by using MTT assay. To conduct the cytotoxicity assay, five tumor cell lines H460, SKOV3, MGC-803, HeLa and T24, and non-tumor cells HL-7702 were selected. In addition, MS analysis detects that **C3** exists in the form of a single nucleus in the solution. Therefore, the molecular weight of **C3** was calculated as a single nucleus in the cytotoxicity test. As shown in Table 2, **L1–L4** and **C1–C3** have no cytotoxicity and low cytotoxicity against five cell lines, respectively, but **C4** possesses considerable cytotoxicity against five cell lines.

The cytotoxicity of the In(III) complexes to human urinary bladder cells (T-24) has a relationship with N-4 substitutions.

Table 2 $IC_{50}$ (μM) values of ligands (**L1–L4**) and In(III) complexes (**C1–C4**)

| | $IC_{50}$ | | | | | |
|---|---|---|---|---|---|---|
| Compounds | H460 | SKOV3 | MGC-803 | HeLa | T24 | HL-7702 |
| **L1** | >100 | >100 | >100 | >100 | >100 | >100 |
| **L2** | >100 | >100 | >100 | >100 | >100 | >100 |
| **L3** | >100 | >100 | >100 | >100 | >100 | >100 |
| **L4** | >100 | >100 | >100 | >100 | 56.78 ± 2.10 | >100 |
| **C1** | >100 | >100 | >100 | >100 | >80 | >100 |
| **C2** | >100 | 43.29 ± 0.36 | >100 | >100 | 52.22 ± 2.51 | >100 |
| **C3** | >50 | 30.80 ± 1.48 | >50 | >50 | 46.11 ± 1.33 | >50 |
| **C4** | 20.25 ± 1.33 | 19.11 ± 1.07 | 11.77 ± 0.88 | 15.22 ± 1.02 | 8.65 ± 0.68 | 21.09 ± 1.01 |
| Cisplatin | 14.89 ± 1.06 | 15.24 ± 1.01 | 13.36 ± 0.61 | 15.66 ± 1.29 | 19.34 ± 1.31 | 15.38 ± 0.56 |

Published on 02 November 2020. Downloaded by Carleton University on 11/21/2020 11:15:23 PM.

By adding an N4-methyl and N4-phenyl group to thiosemicarbazide in **C2** and **C3**, their cytotoxicity (**C2**, $IC_{50}$ = 52.22 ± 2.51 μM and **C3**, $IC_{50}$ = 46.11 ± 1.33 μM) was increased relative to **C1** ($IC_{50}$ > 80 μM), respectively. Besides, by adding two methyl groups to thiosemicarbazide in **C4**, its cytotoxicity against T-24 cells ($IC_{50}$ = 8.65 ± 0.68 μM) was increased about 5-fold relative to **C1** (52.22 ± 2.51 μM). In conclusion, the cytotoxicity of **C1–C3** is much lower than that of cisplatin against T-24 cells ($IC_{50}$ = 19.34 ± 1.31 μM). However, the cytotoxicity of **C4** is higher about 2-fold than that of cisplatin against T-24 cells (19.34 ± 1.31 μM), the cytotoxicity of **C4** is lower than that of cisplatin against normal cells (Table 2).

**2.4.2 Influence of In(III) complexes on cancer cell morphology.** This assay was used to determine the morphological changes of tumor cells after being treated with **C4**. The T-24 cells were treated with **C4** and cisplatin and analyzed for morphological changes. The results showed that the shape of T-24 cells treated with **C4** was more spherical than that of the untreated T-24 cells (Fig. 2A) and T-24 cells treated with cisplatin (Fig. S4†). The apparent change in T24 morphology could be induced by **C4**, suggesting that the tumor growth is inhibited by **C4**.

**2.4.3 In(III) complexes inhibiting the growth of tumor spheroids.** Three dimensional (3D) cell culture is a type of artificially created environment, in which living cells are allowed to grow in a three-dimensional microenvironment with intricate cell–cell and cell–matrix interactions and a complex transport dynamics of nutrients and cells.[29–31] Primarily, the 3D cell spheroid protocol is used to examine the pharmacokinetics and pharmacodynamics of drugs in preclinical trials.[32] We developed a 3D cell culture of T24 cells and treated with **C4** and cisplatin, and then analyzed the growth of the spheroids for time intervals of 0–7 days. The results demonstrated that there is no any change for untreated spheroids, whereas the spheroids treated with **C4** and cisplatin became more compact in structure (Fig. 2B and S4†), which suggested that **C4** can inhibit tumor growth. Besides, **C4** had stronger capacity for keeping the spheroid structure compact than cisplatin.

**2.4.4 In(III) complexes inhibiting metastasis of cancer cells.** Cell migration is a process occurring in cells for tissue development, wound healing, and immune responses. Cell invasion refers to the ability of cells to become motile and travel through the extracellular matrix within a tissue or infiltrate into neighboring tissues. Cell migration and invasion play a vital role in cancer growth and metastasis. To determine cell migration and metastasis in cancer cells and the effect of chemotherapeutic agents on rapidly dividing tissues of healing wounds and migrated cells, wound healing and transwell assay were used.[33–37] We cultured T24 cells in monolayers and pseudo-wounds. The wounded cells were treated with **C4** and cisplatin, and then analyzed for cell growth in time intervals. The cells treated with **C4** showed a slight increase or no increase in migration toward the wounded side, while the cells treated with cisplatin (Fig. S5†) and untreated cells migrated to the wounded side, indicating the inhibition of tumor cell growth by **C4** (Fig. 3A).

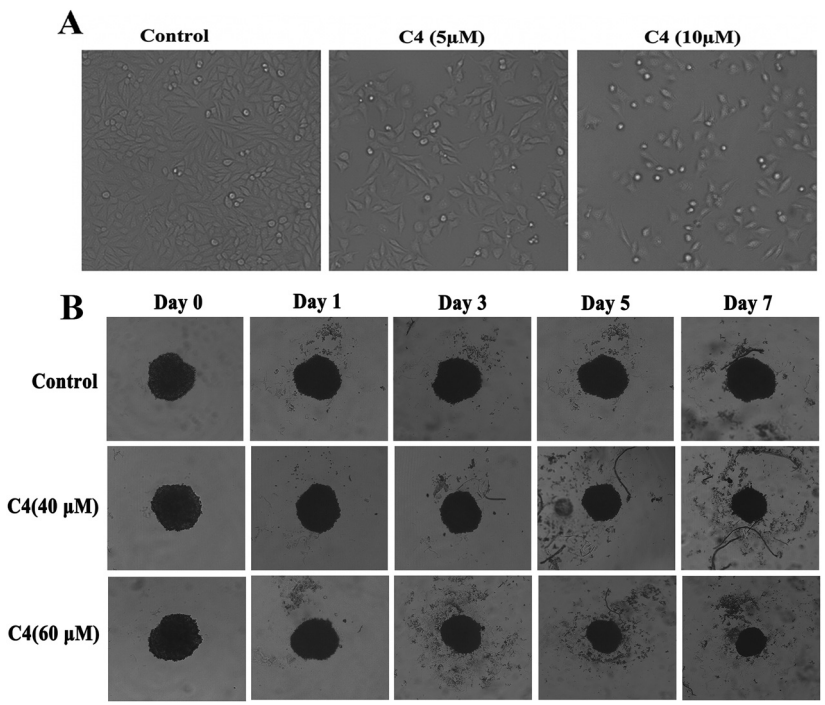


Fig. 2 (A) Analysis of cell morphology in T24 cells after treatment with **C4**. (B) 3D morphology of T24 cell tumor spheroids with vehicles, **C4** with specified concentrations for 8-days.


This journal is © The Royal Society of Chemistry 2020

Published on 02 November 2020. Downloaded by Carleton University on 11/21/2020 11:15:23 PM.

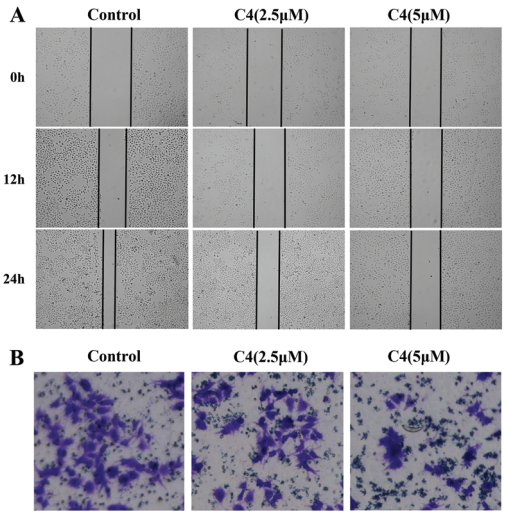


Fig. 3 Analysis of the metastasis in T24 cells after treating with **C4**. (A) Wound healing assay, during a 24-hour wound closure assay, pictures were taken using a time-lapse microscope. (B) A diagram of the transwell insert apparatus used to measure cell migration and invasion cells.

Similarly, a transwell assay was used to determine the inhibition of the invasion of T24. After treatment with **C4** and cisplatin, the invasion in T24 cells treated with **C4** was significantly inhibited relative to that in the untreated cells (Fig. 3B) and cisplatin-treaded cells (Fig. S5†). These suggested that the In(III) complex has the potential to inhibit the metastasis in T24 cells.

### 2.5 Multi-targeting anticancer mechanism of In(III) complexes

Cancer is a complicated and multiple gene/protein involved disease, and drugs that target single proteins could be limited with acquired resistance and adverse side effects.[11–13] Herein, we used anticancer complexes to promote apoptotic and autophagic pathways in cancer cells *via* a multi-target mechanism of actions. **C4** showed higher cytotoxicity against T24 cells, therefore we selected **C4** for further studies.

**2.5.1 Cell cycle regulation.** The flow cytometry data revealed that after treating the T24 cells with **C4** (5 μM and 10 μM) and cisplatin (10 μM) the accumulation of cells in the S-phase increased to 31.12% (5 μM) and 39.19% (10 μM) respectively compared to that of the untreated cells that was 29.33%, suggesting that **C4** arrested the cell cycle in S-phases (Fig. 4A). Furthermore, the accumulation of T-24 cells treated with **C4** significantly increased in the S-phase compared to that of cisplatin-treated cells (Fig. S6†). The cell cycle is regulated by cyclin and cyclin-dependent kinases. Cyclin-A activates CDK2 and promoted the cell cycle progression by inhibition of p21.[38] On the other hand, the oncogenic protein Cdc25A promotes the cell cycle from G1 to the S phase. The degradation of Cdc25A, the expression of p53 and p21, and the inhibition of the CDK2 protein promote the cell cycle in the S-phase.[39] We analyzed the expression and inhibition of these proteins by the western blot technique. The results suggest that after treatment of the T24 cells with **C4** and cisplatin, the expressions of

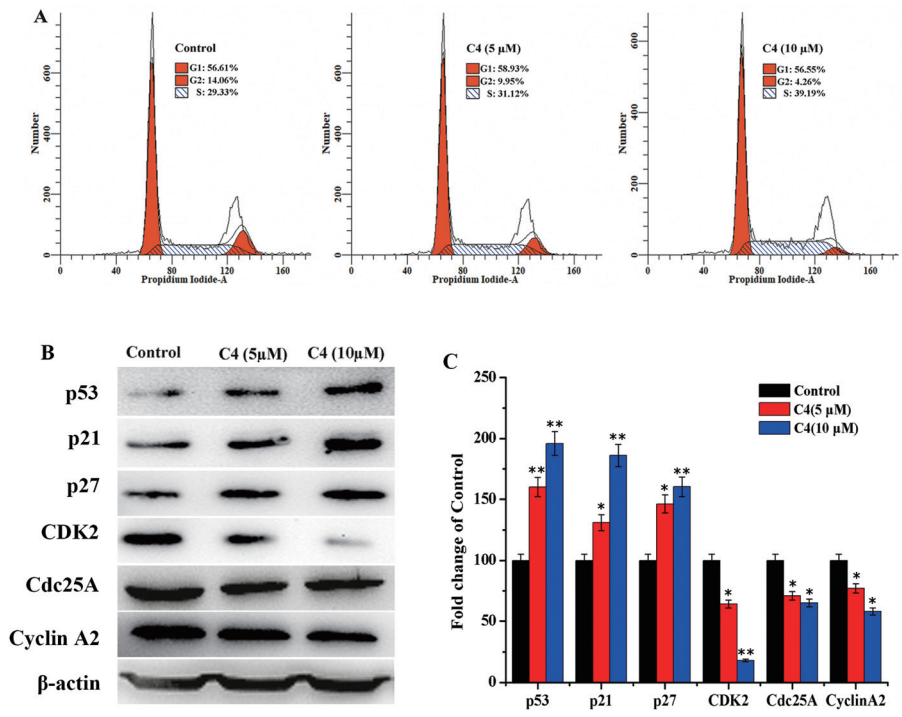


Fig. 4 (A) Effect of the cell cycle of T24 cells treated with **C4** (5 μM and 10 μM) compared with untreated cells. (B) Analysis of the expression level of p53, Cdc25A, Cyclin A2, CDK2, p21, and p27. (C) Percentage expression level of p53, Cdc25A, Cyclin A2, CDK2, p21, and p27; mean ± SD ($n$ = 3): $p$ < 0.05, (**) $p$ < 0.01.

Published on 02 November 2020. Downloaded by Carleton University on 11/21/2020 11:15:23 PM.

CDK2 and Cdc25A in T24 cells were down-regulated, and the expressions of p53 and p21 were up-regulated, which provides considerable indication that **C4** arrests the cell cycle in the S-phase through multiple protein regulations (Fig. 4B, C and S6†).

**2.5.2 Analysis of the mitochondrial-mediated apoptosis.** Apoptosis or programmed cell death is a natural process, regulated by multiple cell signaling pathways.[40] An unbalance in apoptosis in cells or tissues results in cancer progression. Chemotherapy is used to promote apoptosis in tumor cells without affecting healthy cells.[41] We treated the T-24 cells with **C4** (5 μM and 10 μM) and cisplatin (10 μM), and then analyzed apoptosis by using Annexin-V/Propidium Iodide double staining assay by flow cytometry. Fig. 5A shows that the occurrence of apoptosis was increased by 34% (5 μM) and 47% (10 μM) when compared with untreated cells. This experimental data suggested that **C4** induces apoptosis in T24 cells. In addition, **C4** induced more apoptosis in T-24 cells than cisplatin (Fig. S7†).

Chemotherapeutics aims to activate apoptotic cascades and induces mitochondrial-mediated apoptosis in various cancer cells.[42] The Bcl-2 family proteins play a critical role in mitochondrial apoptosis regulations. The Bax inhibited the expression of Bcl-2 and Bcl-xl and activated the expression of the Bad protein, resulting in the release of cytochrome-c from the intermembrane space of the mitochondria into the cytoplasm. Cytochrome-c then makes a complex with procaspase-9 called apoptotic proteases activator factor 1 (APAF-1), which activates cap-3 and leads to cell death.[43–46]

We examined the mitochondrial membrane permeabilization ($\Delta\psi m$) by flow cytometry using a JC-1 assay kit. The cleavage of Cap-9 and Casp-3 and the regulation of Bax, Bcl-xl, Bad, cytochrome C, and APAF-1 were analyzed by western blot. Fig. S3 and S8† show that after the treatment of T24 cells with **C4** and cisplatin, the $\Delta\psi m$ decreased to a varying degree compared to the untreated T24 cells. Western blot data indicated the down-regulation of Bcl-xl and Bcl-2 and the up-regulation of Bax, Bad, cytochrome C, and APAF-1. Similarly, the expression of Cap-9 in T24 cells sufficiently increased (Fig. 5B and C). These results indicated that the activation of mitochondrial apoptosis by the regulations of multiple proteins induce apoptosis in tumor cells.

**2.5.3 Endoplasmic reticulum-mediated stress pathways and ROS generation.** The endoplasmic reticulum has a flat structure containing a network of tubules. It functions as the folding and processing of secretory proteins.[47] The function of the ER is calcium ($Ca^{2+}$) dependent. A high concentration of $Ca^{2+}$ requires regulating the homeostatic condition of the ER.[48,49] The imbalance in ionic or redox state results in ER-stress and accumulation of unfolded proteins.[50] Under the stress condition, the ER-transmembrane receptors, such as protein-kinase-RNA-like ER-kinase (PERK), phosphorylates the eIF2α protein, resulting in the activation of unfolding protein response (UPR).[51,52] On the other hand, phosphorylation of eIF2α by PERK activates the transcriptional factor CCAATEnhancer-binding protein homologous protein (CHOP).[53,54] Under stress conditions, CHOP is overexpressed and activates the pro-apoptotic proteins and leads to mitochondrial-mediated apoptosis.[55]

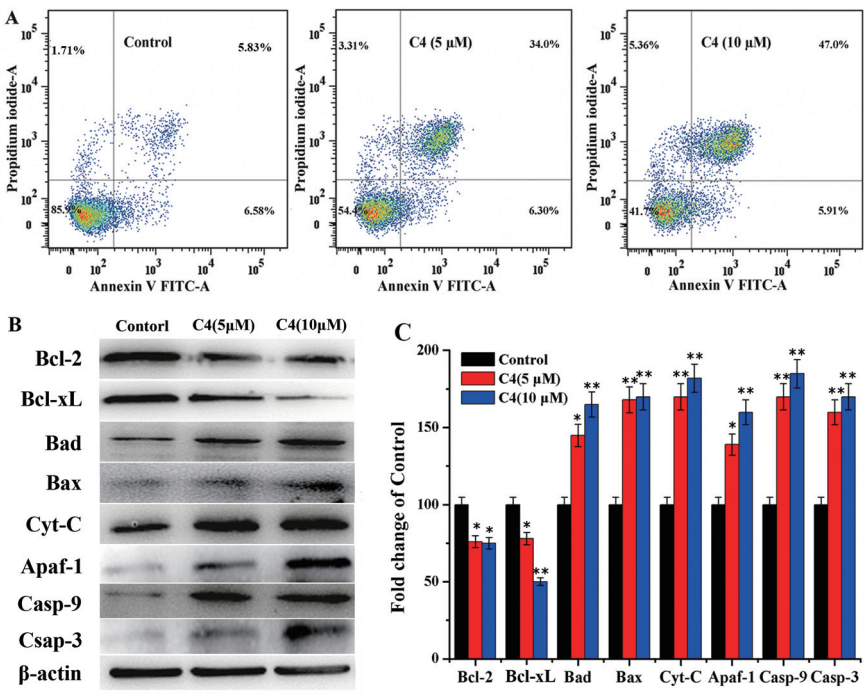


**Fig. 5** (A) Effect of cell apoptosis of T24 cells treated with **C4** (5 μM and 10 μM) compared with untreated cells. (B) Western blot analysis of Apaf-1, Bad, Bax, Bcl-2, Bcl-xl, and Cytochrome C. (C) Percentage expression level of Apaf-1, Bad, Bax, Bcl-2, Bcl-xl, Cytochrome C, Casp-9 and Casp-3 relative to control; mean ± SD ($n$ = 3): $p < 0.05$, (**) $p < 0.01$.


This journal is © The Royal Society of Chemistry 2020

Published on 02 November 2020. Downloaded by Carleton University on 11/21/2020 11:15:23 PM.

Fig. 6B indicates that compared with untreated T24 cells, the treated cells with **C4** showed more deviated peaks, indicating the imbalance of $Ca^{2+}$ concentration in T24 cells. Moreover, the western blot results signified the activation of PERK and eIF2α and the up-regulation of CHOP in T24 cells, which suggested that the ER-stress-mediated apoptosis is activated in T24 cells by **C4** (Fig. 6C and D).

Reactive oxygen species are generated in the mitochondria in a balanced manner. The imbalance in the induction of the mitochondrial ROS leads to dysfunction in cell physiology.[56] Anticancer chemotherapeutics have the ability to generate ROS and induce ER-stress, which could be the potential anticancer agents.[57] After treatment with **C4**, we analyzed the ROS generation in T24 cells using 2′,7′-dichlorodihydrofluorescein diacetate (H2DCFDA) which was oxidized by cellular ROS to 2′,7′-dichlorofluorescein (DCF), while ER-tracker red was used to analyze the ER-stress, which was bound to sulfonylurea receptors in the ER. The T24 cells were incubated with **C4** and clear colonization was observed (Fig. 7). In time intervals, the ROS were found to be more diffused and less colonized, which may indicate the more permeabilization of the ER membrane and the induction of ER-mediated apoptosis.

Besides, the T24 cells were analyzed for ROS generation by flow cytometry. The cells were observed to make deviated peaks from the untreated cells, suggesting the activation of ROS in cancer cells treated with **C4** (Fig. 6A). Furthermore, the **C4**-treated cells significantly increased the ROS and ER-stress than cisplatin-treated cells (Fig. S9 and S10†).

**2.5.4 Regulation of the telomerase reverse transcriptase by C4.** The MYC proto-oncogene encodes a transcription factor (c-Myc) that plays a key role in the control of cell proliferation and differentiation.[58] c-Myc activates telomerase by the

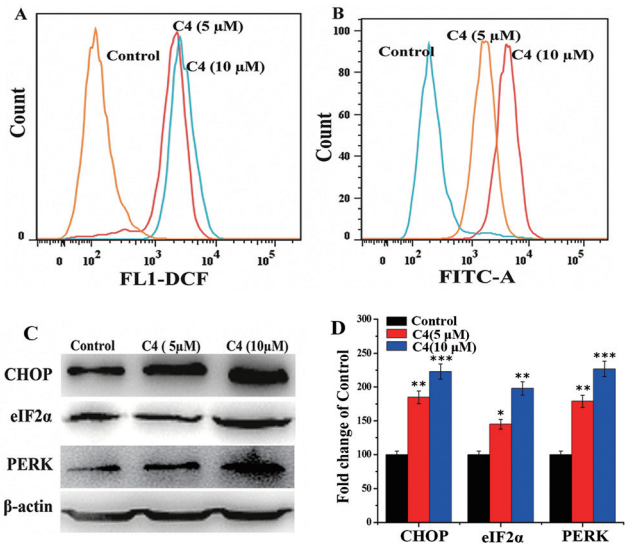


Fig. 6 T24 cells treated with **C4** and analysis of (A) ROS concentration, (B) $Ca^{2+}$ concentration in T24 cells, (C) western blot analysis of PERK, eIF2α and CHOP in T24 cells, (D) graphical presentation of the expression level of PERK, eIF2α, and CHOP; mean ± SD ($n$ = 3): $p < 0.05$, (**) $p < 0.01$, (***) $p < 0.001$.

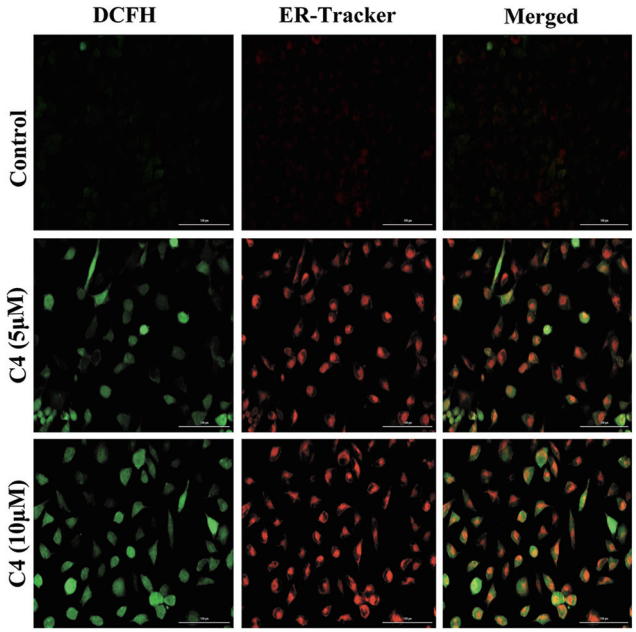


Fig. 7 Generation of ROS by using 2′,7′-dichlorofluorescein (DCF) and analysis of ER-tracker red by binding to sulfonylurea receptor in the ER.

expression of its catalytic subunit, telomerase reverse transcriptase (TERT).[59] Human telomerase reverse transcriptase (hTERT) is upregulated in most cancer cells but do not express in normal cells.[60] Myc is thus viewed as a promising target for anti-cancer drugs.[61] We analyzed the expressions of hTERT and c-Myc by the western blotting technique. After the T24 cells were treated with **C4** (5 μM and 10 μM) and cisplatin (10 μM), the expression of these proteins was remarkably inhibited (Fig. 8A–C and S11†), which suggested that **C4** and cisplatin inhibit the telomerase activities in T-24 cells. However, **C4** had stronger capacity for inhibiting telomerase activity than cisplatin.

**2.5.5 Induction of the MAPK apoptotic pathway by C4.** Mitogen-activated protein kinase (MAPK) also called the extracellular signal-regulated kinases (ERK) pathway is a chain of proteins in the cell that communicates a signal from a receptor on the surface of the cell to the DNA in the nucleus of the cell,[62,63] that regulated apoptotic and autophagic pathways in cells.[64] An extracellular mitogen is phosphorylated, which helps the activation of MAPKs. MAPKs further activate the transcriptional factors such as cyclins and cyclin-dependent kinases.[65] P38MAPKs, ERKs, and JNKs are the isoforms of MAPK family proteins.[66–68] In response to cellular stress, these proteins are activated by phosphorylation and their cell functions, including apoptosis, are regulated.[69] On the other hand, protein kinase B (AKT) is a cell survival protein that inhibits apoptosis and promotes growth factor-mediated cell survival. AKT phosphorylates the BAD-protein, isolates from the Bcl-2/Bcl-xl complex and inhibits its pro-apoptotic function. Numerous compounds that targeted the MAP/ERK pathway are considered to be the potential anticancer chemotherapeutics.[70,71] T24 cells were treated with **C4** (5 μM and 10 μM) and then analyzed by western blot for the expressions of p-P38, p-JNKs, p-ERK, and p-Akt-1 pro-

Published on 02 November 2020. Downloaded by Carleton University on 11/21/2020 11:15:23 PM.

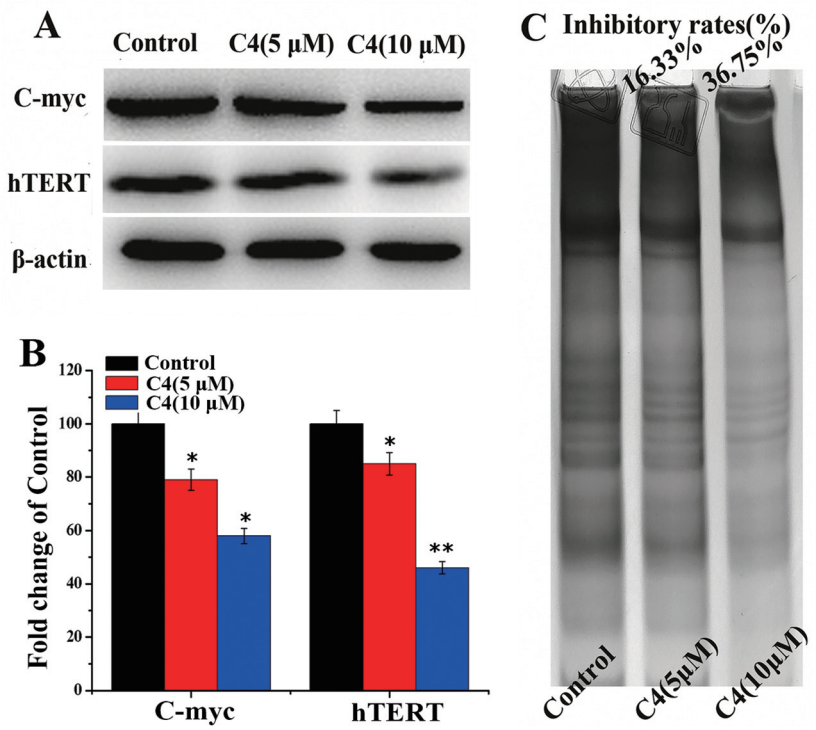


**Fig. 8** (A) Western blot analysis of c-myc and hTERT in T24 cells treated with **C4** for 24 h, (B) densitometric analysis of hTERT and c-myc proteins, (C) the influence on the telomerase activity in the T24 cells treated with **C4**; mean ± SD ($n$ = 3): $p < 0.05$, (**) $p < 0.01$.

teins. As shown in Fig. 9A and B, the expressions of p-P38, p-JNK, and p-ERK were upregulated, while that of p-Akt-1 was down-regulated, indicating the activation of MAPK-mediated apoptosis in T24 cells. These results indicated that both **C4** and cisplatin induce apoptosis and autophagy in T24 cells and are associated with MAPK and Akt signaling pathways. However, **C4** possessed higher activity than cisplatin (Fig. S12†).

**2.5.6 Induction of the autophagic pathway by C4.** The cytosolic protein, namely, the microtubule-associated tubule 1A/1B light chain-3 protein (LC3) is associated with autophagy. The LC3 is phosphorylated in the cytosol to form a complex (LC3-II) and induce cell autophagy.[72] Furthermore, an autophagic receptor, sequestosome 1 (SQSTM1/p62), interacting with LC3, is constantly degraded during autophagy and eliminates autophagic-dependent substances.[73] Besides, beclin-1, an autophagic-associated protein, interacts with Bcl-2 and Bcl-xl proteins and regulates the cell death and survival and acts as a crosslink between apoptosis and autophagy.[74] The treated T24 cells were analyzed by western blot for LC3-II, p62, and beclin-1 expression. The western blot data showed that the LC3-II and beclin-1 were up-regulated, while the p62 was down-regulated (Fig. 10A–C). These results not only confirmed the activation

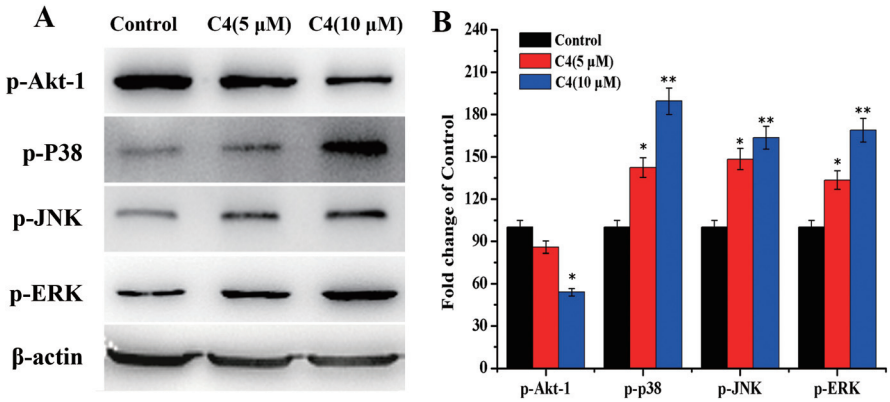


**Fig. 9** (A) Western blot analysis of Akt1/2 and P38, (B) analysis of the expression percentage level of Akt1/2 and P38; mean ± SD ($n$ = 3): $p < 0.05$, (**) $p < 0.01$.


This journal is © The Royal Society of Chemistry 2020

Published on 02 November 2020. Downloaded by Carleton University on 11/21/2020 11:15:23 PM.

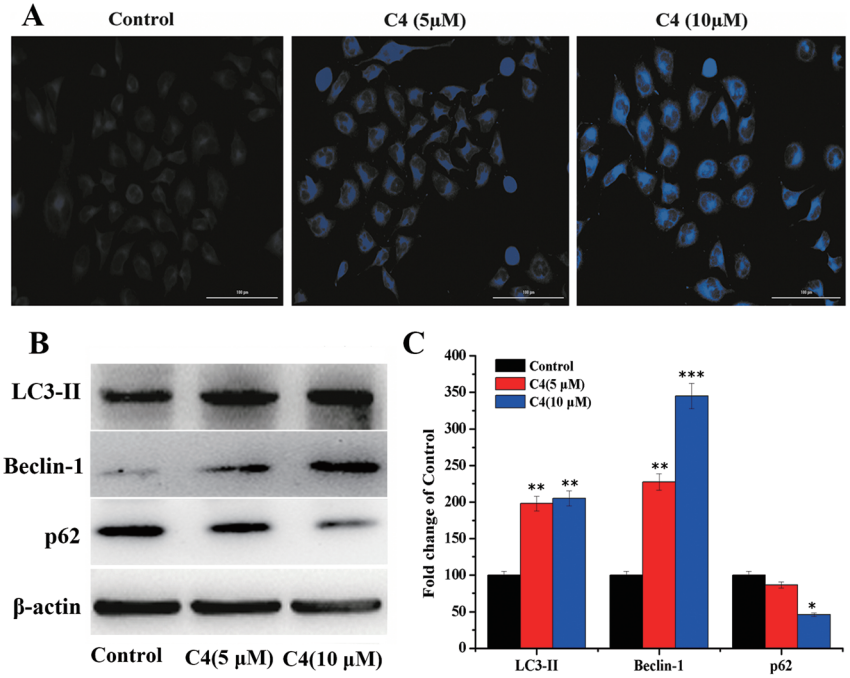


**Fig. 10** (A) Morphological analysis of the induction of autophagy after treated with In(III) complex **C4**, (B) western blot analysis of the expression level of LC3-II, Beclin-1 and P62, relative to the control, (C) graphical presentation of the percentage expression level of LC3-II, Beclin-1 and P62; mean ± SD ($n$ = 3): $p < 0.05$, (**) $p < 0.01$, and (***) $p < 0.001$.

of autophagy in T24 cells but also revealed the crosstalk of autophagy with apoptosis. In addition, **C4** had stronger capacity for autophagy modulation than cisplatin (Fig. S13†).

## 3 Discussion

Over the past several decades, the characterization of novel In (III) thiosemicarbazide complexes has been extensively studied and investigated for their biological applications,[22,23,75] but only a few anticancer In thiosemicarbazide complexes have been investigated.[76,77] To develop potential non-Pt anticancer agents, In complexes are worthwhile to be deeply studied. Herein, we have been successful to synthesize four novel In bis (thiosemicarbazide) complexes for the first time. Interestingly, previous studies revealed that the anticancer activity of metal thiosemicarbazide complexes is directly related to the anti-cancer activity of thiosemicarbazides. Indeed, the results of In bis(thiosemicarbazide) complexes confirmed the rule again. The lipophilic groups attached to the thiosemicarbazide played an important role in increasing the anti-cancer activity of the In complexes. When the H atom(s) in the N4 location of the thiosemicarbazide was replaced by more lipophilic groups, the $IC_{50}$ value of **C4** is lower than that of **C1–C3** (Table 1). Therefore, to regulate the anticancer properties of In complexes, we can modify the lipophilic group(s) of the thiosemicarbazide.

Cisplatin is commonly used to treat various solid cancers, but it produced severe side effects because it damaged DNA. To overcome the deficiency of Pt-based anticancer agents, on the one hand, inorganic medicine researchers attempted to design multi-target metal agents; on the other hand, they designed metal agents based on non-DNA targets or other anti-cancer mechanisms. As a matter of fact, In bis(thiosemicarbazide) complexes acted against cancer cells by multiple approaches, including working on proteins related to cancer and other anticancer mechanisms. It is known that the main cause of cancer death is the fact that cancer cells can spread to other organs and tissues in the advanced stage of cancer. It is highly challenging for designing a metal agent that inhibits tumor metastasis. Excitingly, the In bis(thiosemicarbazide) complex can be effective in inhibiting metastasis of cancer cells. Obviously, the In bis(thiosemicarbazide) complex has shown promise for the development as a multi-functional and multi-targeting anticancer lead metal drug.

## 4 Experiments

### 4.1 Materials

All the chemicals used were in a highly pure form. $H_2O$ used in all reactions was distilled prior to use. 2,6-Diacetylpyridine and thiosemicarbazide were provided by Energy Chemical Company Shanghai, (Shanghai, China). Single crystals were analyzed using a Bruker APEX-II CCD diffractometer. UV-Vis spectra were recorded using a UV-Vis spectrophotometer (Shimadzu, UV-2600). All the cell lines (H460, SKOV3, 803, T24 and HeLa and non-tumor cells HL-7702) were provided by the Shanghai

Published on 02 November 2020. Downloaded by Carleton University on 11/21/2020 11:15:23 PM.

Institute of Biological Sciences. All the antibodies used in western blot were provided by Abcam (Cambridge, UK).

### 4.2 Synthesis of ligands (L1–L4)

Ligands **L1–L4** were synthesized by the reflux method. As shown in Scheme S1,† 5 mM 2,6-diacetylpyridine and thiosemicarbazides (**L1**), 5 mM 2,6-diacetylpyridine and 4-methyl-3-thiosemicarbazide (**L2**), 5 mM 2,6-diacetylpyridine and 4-phenyl-3-thiosemicarbazide (**L3**), and 5 mM 2,6-diacetylpyridine 4,4-dimethyl-3-thiosemicarbazide (**L4**) were stirred in $C_2H_5OH$ for 3 h at 65 °C. The ligands were precipitated and filtered. **L1–L4** were characterized by infrared spectroscopy, electrospray ionization mass spectrometry (ESI-MS), and $^1$H NMR (ESI†).

**L1**: 2,6-diacetylpyridine thiosemicarbazide; yield: 60.6%. Anal. calcd[1] for $C_{11}H_{15}N_7S_2$: 309.414, C, 42.72; H, 4.88; N, 31.68; S, 20.72. Found: C, 42.71; H, 4.89; N, 31.71; S, 20.69. IR, $cm^{-1}$: 3388 (s, amide), 3261 (s, NH), 3122 (m, aromatic hydrogen), 1663 (s, aromatic), 1570, 1503, 1454, 1379 (m, C═N), 1280, 1204, 1169, 1102 (s, thioamide), 860, 818, (m, C–H), 559, 509 (m, C═S). $^1$H NMR (400 MHz, DMSO) $\delta$ 10.33 (s, 2H), 8.49–8.36 (m, 4H), 8.17 (s, 2H), 7.79 (t, $J$ = 7.9 Hz, 1H) and 2.45 (s, 6H). ESI + MS: $m/z$ = 310.09 $[M + H]^+$.

**L2**: 2,6-diacetylpyridine 4-methyl-3-thiosemicarbazide; yield: 56.7%. Anal. calcd[1] for $C_{13}H_{19}N_7S_2$: 337.46, C, 46.26; H, 5.67; N, 29.05; S, 19.00. Found: C, 46.28; H, 5.68; N, 29.08; S, 18.97. IR, $cm^{-1}$: 3409, 3299 (s, amide), 3299 (s, NH), 2936 (m, aromatic hydrogen), 1692 (s, aromatic), 1549, 1513, 1534 (m, C═N), 1494, 1447, 1392, 1256, 1175 (s, thioamide), 851, 811, 754 (m, C–H), 693, 576 (m, C═S). $^1$H NMR (400 MHz, DMSO) $\delta$ 10.35 (s, 2H), 8.64 (q, $J$ = 4.6 Hz, 2H), 8.41 (d, $J$ = 7.9 Hz, 2H), 7.84 (t, $J$ = 7.9 Hz, 1H), 3.06 (d, $J$ = 4.6 Hz, 6H) and 2.44 (s, 6H). ESI + MS: $m/z$ = 360.10 $[M + Na]^+$.

**L3**: 2,6-diacetylpyridine 4-phenyl-3-thiosemicarbazide; yield: 49.8%. Anal. calcd[1] for $C_{23}H_{23}N_7S_2$: 461.61, C, 59.84; H, 5.02; N, 21.33; S, 13.89. Found: C, 59.85; H, 5.03; N, 21.26; S, 13.87. IR, $cm^{-1}$: 3544 (s, amide), 3299 (s, NH), 1596, 1534 (m, aromatic hydrogen), 1494, 1447 (s, aromatic), 1320, 1256 (m, C═N), 1175 (s, thioamide), 851, 811 (m, C–H), 754, 693, 576 (m, C═S). $^1$H NMR (400 MHz, DMSO) $\delta$ 10.22 (s, 2H), 8.05 (q, $J$ = 7.8 Hz, 2H), 7.92–7.85 (m, 3H), 2.45 (s, 6H) and 1.56 (s, 18H). ESI + MS: $m/z$ = 484.13 $[M + Na]^+$.

**L4**: 2,6-diacetylpyridine 4,4-dimethyl-3-thiosemicarbazide; yield: 45.9%. Anal. calcd[1] for $C_{15}H_{23}N_7S_2$: 365.520, C, 49.28; H, 6.34; N, 26.82; S, 17.54. Found: C, 49.30; H, 6.35; N, 26.84; S, 17.51. IR, $cm^{-1}$: 3462, 3269 (s, amide), 2971 (s, NH), 1696, 1574 (m, aromatic hydrogen), 1504, 1448 (s, aromatic), 1358, 1242 (m, C═N), 1113, 1017 (s, thioamide), 817 (m, C–H), 698, 642, 596 (m, C═S), $^1$H NMR (400 MHz, DMSO-d6) $\delta$ 9.50 (s, 1 H), 8.52 (dd, $J$ = 15.5, 2.4 Hz, 2 H), 3.77–3.63 (m, 4 H), 3.22 (q, $J$ = 7.4 Hz, 2 H), 2.36 (s, 3 H), 1.91 (s, 4 H), 1.22 (t, $J$ = 7.4 Hz, 3 H). ESI + MS: $m/z$ = 366.42 $[M + H]^+$.

### 4.3 Synthesis of In(III) complexes (C1–C4)

**C1–C4** were prepared by treating the ligands **L1–L4** (0.10 mmol) with $InCl_3$ (0.10 mmol) in methanol (2.5 mL) under solvothermal conditions at 80 °C for 2 days. **C1–C4** were characterized by X-ray crystallography, infrared spectroscopy and electrospray ionization mass spectrometry (ESI-MS) (ESI†).

$[In(L1)Cl_2]$ (**C1**): yield: 62.5%, Anal. calcd for $C_{11}H_{14}Cl_2InN_7S_2$: C, 26.13; H, 2.85; N, 19.84; S, 12.97. Found: C, 26.73; H, 2.86; N, 19.85; S, 12.95. IR, $cm^{-1}$: IR, $cm^{-1}$: 3348 (s, amide), 3311 (s, NH), 3384, 3193, 2345 (s, aromatic), 1622 (s, C═N), 1586, 1543, 1399, 1363 (s, thioamide), 1296, 1207, 1011, 986 (m, C–H), 804, (m, C═S), 787, 646, 574. ESI + $m/z$: $C_{11}H_{14}Cl_2InN_7S_2$, 421.97 $[M - 2Cl]^+$.

$[In(L2)Cl_2]$ (**C2**): yield: 59.1%, Anal. calcd for $C_{13}H_{18}Cl_2InN_7S_2$: C, 30.00; H, 3.28; N, 18.81; S, 12.30. Found: C, 29.95; H, 3.29; N, 18.82; S, 12.28. IR, $cm^{-1}$: IR, $cm^{-1}$: 3398 (s, amide), 3334 (s, NH), 2928, 2345, (s, aromatic), 1637, 1563, 1512 (s, C═N), 1326 (s, thioamide), 1392, 1366, 1327, 1274, 1200, 1045 (m, C–H), 804, 740, 708, (m, C═S), 651. ESI + $m/z$: $C_{13}H_{18}Cl_2InN_7S_2$, 450.00 $[M - 2Cl]^+$.

$[In(L3)Cl]_2$ (**C3**): yield: 54.7%, Anal. calcd for $C_{46}H_{42}Cl_2In_2N_{14}OS_4$: C, 45.22; H, 3.88; N, 16.05; S, 10.49. Found: C, 45.22; H, 3.88; N, 16.06; S, 10.48. IR, $cm^{-1}$: IR, $cm^{-1}$: 3413 (s, amide), 3304 (s, NH), 1677, 1593, 1481 (s, C═N), 1454 (s, thioamide), 1367, 1322, 1165, 1189, 1074 (m, C–H), 807 (m, C═S), 621, 508. ESI + $m/z$: $C_{23}H_{21}ClInN_7S_2$, 574.03 $[M - Cl]^+$.

$[In(L4)Cl_2]$ (**C4**): yield: 49.2%, anal. calcd for $C_{16}H_{25}Cl_3InN_7S_2$: C, 32.68; H, 4.20; N, 17.78; S, 11.63. Found: C, 32.68; H, 4.21; N, 17.79; S, 11.61. IR, $cm^{-1}$: IR, $cm^{-1}$: 3417 (s, amide), 2927, 2351, (s, NH), 1619, 1567, 1499 (s, aromatic), 1464 (s, C═N), 1377 (s, thioamide), 1316, 1297, 1249, 1167, 1113 (m, C–H), 809 (m, C═S), 761, 437. ESI + $m/z$: $C_{15}H_{23}Cl_2InN_7S_2$, 478.03 $[M - 2Cl]^+$.

### 4.4 X-Ray crystallography of In(III) complexes

A single crystal each of **C1–C4** was selected to analyze using a Bruker APEX-II CCD diffractometer. The crystals were kept at 296.15 K during the data collection. Using Olex2, the structure was solved with the XS structure solution program using direct methods and refined with the XL refinement package using Least Squares minimization. The data in the CIF format were input at the Cambridge crystallographic data center under the CCDC number 1961553 for **C1**, 1961543 for **C2**, 1961545 for **C3**, and 1961546 for **C4**.†

### 4.5 MTT assay

H460, SKOV3, MGC-803, HeLa, T24 and non-tumor cell HL-7702 were analyzed to determine the cytotoxicity of **C1–C4**. Each of the cells was grown in Dulbecco's modified Eagle's medium (DMEM) at 37 °C and under 5% $CO_2$ conditions separately. **C1–C4** were dissolved into DMSO and then diluted with PBS. The amount of DMSO in **C1–C4** solution is lower than 1%. The stability of In(III) complexes in solution was checked by using UV. Cisplatin was directly dissolved into PBS.

To determine the cytotoxicity of **C1–C4**, we used 3-(4,5-dimethylthiazol-2-yl)-2,5-diphenyltetrazolium bromide (MTT) assay. To initiate this assay, 96-well plates were used. 180 μL of each of the cell solution was added to each well and incubated for 24 h. The cells were then treated with different concen-

 This journal is © The Royal Society of Chemistry 2020

Published on 02 November 2020. Downloaded by Carleton University on 11/21/2020 11:15:23 PM.

trations of **C1–C4**, and cisplatin for 48 h. 10 μL of MTT was added to each well and incubating for 4 h. The media were removed, 100 μL of DMSO was added to each well and analyzed using enzyme labeling instruments to determine the $IC_{50}$ values of In(III) complexes against tumor cells.

### 4.6 Cellular uptake assay

Inductively coupled plasma (ICP-MS) was used to determine the distribution of "In" in cancer cells. T24 cells were cultured and treated with In complexes **C1**, **C2**, **C3**, and **C4**, and cisplatin for 24 h. The mitochondrial membrane fraction, nuclear fraction and cytoplasmic fraction were separated and extracted using the NE-PER assay protocol. The cell extract each for mitochondrial fraction, nuclear fraction and the cytoplasmic fraction was stored at −80 until analyzed using ICP-MS.

### 4.7 Cell morphology analysis

Tumor cells T24 with concentrations of $1 \times 10^5$ cells per mL were cultured in six-well plates and incubated at 37 °C and under 5% $CO_2$ environments. The cells were then treated with **C4** and cisplatin for 24 h and were observed under a bright-field microscope.

### 4.8 Tumor spheroid growth inhibition assay

The three-dimensional (3D) spheroid assay was used to analyze the physiological characteristics of cells. To perform this protocol, 96-well microtiter plates were used. Agarose-DMEM solution (1.5% (wt/v)) was sterilized and heated to 80 °C. Agarose solution (50 μL) was added to each well and allowed to solidify. T24 cells with a concentration of $1 \times 10^3$ cells per well were grown on the upper lips of cell culture plates and incubated at 37 °C, and under a 5% $CO_2$ atmosphere. After 72 h, one of each T24 cell spheroid was transferred into each agarose coated well and allowed to settle. Each T24 cell spheroid except the control was treated with **C4** and cisplatin and then analyzed for spheroid growth every 48 h for up to seven days.

### 4.9 Wound healing assay

Wound healing assay was made to determine the efficacy of the In(III) complex **C4** against T-24. The cells were seeded in 6-well plates and allowed to grow in monolayers. The monolayered cells were wounded using a sterile 200 μL pipette tip, generated a clean wound area and washed with PBS. The cells were incubated **C4** and cisplatin for 24 h and analyzed under a bright field microscope.

### 4.10 Cell invasion assay

To measure the capacity of cell motility and invasiveness toward chemotherapeutics, we used cell invasion assay. T-24 cells were cultured in 24-well plates and placed in the Transwell chamber in 24-well plates. 100 μL of Matrigel (a serum-free media) with and without treated with **C4** and cisplatin was added to the upper chambers and incubated at 37 °C for 24 h. We added 750 μL of culture media to the lower chambers and placed 200 μL of T24 cell solution ($2.5 \times 10^5$ $ml^{-1}$) in serum-free chambers, and then placed the transwell into lower chambers and incubated at 37 °C for 15 h. The media were removed and washed with PBS. The cells were fixed with 3.7% formaldehyde, washed and permeabilized with 100% methanol. The cells were stained with Giemsa for 15 min, washed and analyzed under a bright field microscope.

### 4.11 Cell cycle analysis

T24 cells with a concentration of $1 \times 10^5$ cell per mL were cultured in DMEM and incubated at 37 °C and under 5% $CO_2$ conditions for 12 h. The cells were treated with **C4** and cisplatin for the next 24 h, collected by centrifugation, washed with bovine phosphate serum (PBS) and fixed with cold ethanol followed by overnight storage at −20 °C. The cells were washed with PBS and incubated with DNA-free RNase-A for 30 min. 10 μL of 1 mg $mL^{-1}$ propidium iodide solution was added to each cell's solution and analyzed by flow cytometry.

### 4.12 Cell apoptosis assay

We cultured the T24 cell in DMEM and treated it with **C4** and cisplatin. The double staining (Annexin-V and PI) protocol was used to determine apoptosis in T-24 cells. The cells were collected by centrifugation, incubated in 200 μL of Annexin-V binding buffer, and 5 μL of Annexin-V, added to each cell's tube, excepting the PI control for 20 min and 37 °C in the dark. After 20 min, 300 μL of 1×-Annexin-V binding buffer was added to each tube, followed by 4 μL of PI to each cell's tube, except the Annexin-V control and incubated for 20 min in the dark at 37 °C. The cells were then analyzed for apoptosis using flow cytometry.

### 4.13 Measurements of mitochondrial membrane potential $\Delta\psi m$

To determine the mitochondrial membrane potential ($\Delta\psi m$), we used a 5,5′,6,6′-tetrachloro-1,1′,3,3′-tetraethyl-benzimidazolylcarbocyanine iodide (JC-1) assay kit. T-24 cells were seeded in 6-well cell plates, treated with **C4** and cisplatin then incubated for 15 h at 37 °C. The cells were then collected by centrifugation, washed with PBS and incubated with 500 μL of JC-1 solution in the dark. The cells were then analyzed for $\Delta\psi$m using flow cytometry.

### 4.14 Imagining of the ROS in the endoplasmic reticulum

$2 \times 10^6$ cells per well T24 cells were cultured in six-well plates on poly-L-lysine-coated coverslips in heat deactivated complete RPMI, treated with **C4** and cisplatin for 6 hours and collected by centrifugation. The cells were washed with pre-warmed PBS, followed by incubation with 25 μM pre-warmed 2′,7′-dichlorodihydro-fluorescein diacetate (H2DCF-DA) for 20 min at 37 °C. 1 μM pre-warmed ER-Tracker Red was added to the cells and incubated for 15 min and washed with PBS. The cells were mounted onto slides and analyzed using confocal microscopy. A 20× objective lens was acquired to take images and processed using the Zeiss FLUOVIEW Viewer software.

Published on 02 November 2020. Downloaded by Carleton University on 11/21/2020 11:15:23 PM.

### 4.15 Analysis of the intracellular $Ca^{2+}$ ion

The Fluo-3 AM assay protocol was used to determine the intracellular $Ca^{2+}$. T24 cells were cultured in six-well cell plates and incubated at 37 °C for 24 h. The cells were then incubated with **C4** and cisplatin for another 24 h. The cells were then incubated with fluo-3 AM for $Ca^{2+}$ staining and analyzed using flow cytometry.

### 4.16 Western blot analysis

T-24 cells were cultured and treated with **C4** and cisplatin for 24 h. The cells were collected by centrifugation and washed thrice with cold PBS. Radioimmunoprecipitation (RIPA) assay buffer was used to lyse the treated T24 cells. To determine the protein concentration in the T-24 cell's lysate, we used the bicinchoninic acid (BCA) assay protocol. 10% SDS-polyacrylamide gel electrophoresis was used to separate the equal amount of total proteins. The proteins were then transferred to poly(vinylidene difluoride) membranes (Millipore, MA, USA) and blocked in 5% fat-free milk for 30 min and washed with TBST (20 mM Tris, 150 mM NaCl, pH 8.0 and 0.05% tween 20) three times. The membrane was then incubated overnight in primary antibodies at 4 °C, washed thrice with TBST and incubated in secondary antibodies for two hours at room temperature. Amersham ECL plus (western blotting detecting reagent) was used to detect the immunoreactivity of the proteins.

## 5 Statistical analyses

All the experiments carried out in this study were repeated 3 to 5 times. Student's *t*-test was used to evaluate the significance of differences measured. Results were expressed as mean ± SD and considered to be significant when $p < 0.05$.

## 6 Conclusions

The four In(III) complexes revealed the chemotherapeutic effect through multi-target mechanisms. The efficacy of the In(III) complexes was structure-dependent and increased with modifications of the N-4 position of the ligand thiosemicarbazides. **C4** exhibited more potent antitumor activity against T24 cells, not only inhibited the tumor by multi-targeted mechanism but also prevented the tumor invasion and metastasis in T24 cells. In conclusion, In(III) complexes derived from thiosemicarbazides could be the promising multi-target anticancer metal lead drug.

## Abbreviations

| | |
|---|---|
| In | Indium |
| T24 | Human bladder cancer cells |
| 3D cell culture | 3-Dimensional cell culture |
| $\Delta\psi m$ | Mitochondrial depolarization |
| AKT | Protein kinase-B |
| PERK | Protein-kinase-RNA-like |
| ROS | Reactive oxygen species |
| MAPK | Mitogen-activated protein kinase |
| LC3 | Microtubule-associated protein 1A/B-light chain 3 |

## Conflicts of interest

There are no conflicts of interest to declare.

## Acknowledgements

This work received financial support from the Natural Science Foundation of Guangxi (2017GXNSFEA198002 and AD17129007), the Guangxi "Bagui" Scholar Program to HB Sun, and the High-Level Innovation Team and Distinguished Scholar Program of Guangxi Universities to F Yang.

## References

1 R. L. Siegel, K. D. Miller and A. Jemal, *CA Cancer J. Clin.*, 2016, **66**, 7–30.
2 A. Farce, C. Loge, S. Gallet, N. Lebegue, P. Carato, P. Chavatte, P. Berthelot and D. Lesieur, *J. Enzyme Inhib. Med. Chem.*, 2004, **19**, 541–547.
3 K. D. Miller, R. L. Siegel, C. C. Lin, A. B. Mariotto, J. L. Kramer, J. H. Rowland, K. D. Stein, R. Alteri and A. Jemal, *CA Cancer J. Clin.*, 2016, **66**, 271–289.
4 M. Galanski, M. A. Jakupec and B. K. Keppler, *Curr. Med. Chem.*, 2005, **12**, 2075–2094.
5 T. C. Johnstone, G. Y. Park and S. J. Lippard, *Anticancer Res.*, 2014, **34**, 471–476.
6 V. Brabec and J. Kasparkova, *Drug Resist. Updates*, 2005, **8**, 131–146.
7 P. C. Bruijnincx and P. J. Sadler, *Curr. Opin. Chem. Biol.*, 2008, **12**, 197–206.
8 J. Zhang, L. Wang, Z. Xing, D. Liu, J. Sun, X. Li and Y. Zhang, *Adv. Anticancer Agents Med. Chem.*, 2010, **10**, 272–282.
9 M. B. Shahsavani, S. Ahmadi, M. D. Aseman, S. M. Nabavizadeh, M. Rashidi, Z. Asadi, N. Erfani, A. Ghasemi, A. A. Saboury and A. Niazi, *J. Photochem. Photobiol., B*, 2016, **161**, 345–354.
10 J. Qi, S. Liang, Y. Gou, Z. Zhang, Z. Zhou, F. Yang and H. Liang, *Eur. J. Med. Chem.*, 2015, **96**, 360–368.
11 R. G. Fu, Y. Sun, W. B. Sheng and D. F. Liao, *Eur. J. Med. Chem.*, 2017, **136**, 195–211.
12 W. Zheng, Y. Zhao, Q. Luo, Y. Zhang, K. Wu and F. Wang, *Curr. Top. Med. Chem.*, 2017, **17**, 3084–3098.
13 H. Singh, N. Kinarivala and S. Sharma, *Adv. Anticancer Agents Med. Chem.*, 2019, **19**, 842–874.

 This journal is © The Royal Society of Chemistry 2020

Published on 02 November 2020. Downloaded by Carleton University on 11/21/2020 11:15:23 PM.

14 M. Asadi, N. Savaripoor, Z. Asadi, M. H. Ghatee, F. Moosavi, R. Yousefi and M. Jamshidi, *Spectrochim. Acta, Part A*, 2013, **101**, 394–399.
15 P. Heffeter, V. F. Pape, E. A. Enyedy, B. K. Keppler, G. Szakacs and C. R. Kowol, *Antioxid. Redox Signaling*, 2019, **30**, 1062–1082.
16 S. Arora, S. Agarwal and S. Singhal, *Int. J. Pharm. Sci.*, 2014, **6**, 3–24.
17 D. S. Kalinowski, P. Quach and D. R. Richardson, *Future Med. Chem.*, 2009, **1**, 1143–1151.
18 F. Gao, Y. Zhou and H. Liu, *Curr. Org. Chem.*, 2017, **21**, 1530–1566.
19 F. A. French and E. J. Blanz Jr., *Cancer Res.*, 1965, **25**, 1454–1458.
20 T. Khan, R. Ahmad, I. Azad and S. Raza, *Comput. Biol. Chem.*, 2018, **75**, 178–195.
21 J. A. Pardoe and A. J. Downs, *Chem. Rev.*, 2007, **107**, 2–45.
22 J. Chan, A. L. Thompson, M. W. Jones and J. M. Peach, *Inorg. Chim. Acta*, 2010, **363**, 1140–1149.
23 C. Paek, S. O. Kang, J. Ko and P. J. Carroll, *Organometallics*, 1997, **16**, 4755–4758.
24 A. Molter and F. Mohr, *Dalton Trans.*, 2011, **40**, 3754–3758.
25 E. M. Bavin, R. J. Rees, J. M. Robson, M. Seiler, D. E. Seymour and D. Suddaby, *J. Pharm. Pharmacol.*, 1950, **2**, 764–772.
26 O. Koch and G. Stuttgen, *Naunyn-Schmiedebergs Arch. Exp. Pathol. Pharmakol.*, 1950, **210**, 409–423.
27 A. Khan, J. P. Jasinski, V. A. Smolenski, E. P. Hotchkiss, P. T. Kelley, Z. A. Shalit, M. Kaur, K. Paul and R. Sharma, *Bioorg. Chem.*, 2018, **80**, 303–318.
28 F. Yang and H. Liang, *Future Med. Chem.*, 2018, **10**, 1881–1883.
29 G. R. Souza, J. R. Molina, R. M. Raphael, M. G. Ozawa, D. J. Stark, C. S. Levin, L. F. Bronk, J. S. Ananta, J. Mandelin and M. M. Georgescu, *Nat. Nanotechnol.*, 2010, **5**, 291.
30 F. Pampaloni, E. G. Reynaud and E. H. K. Stelzer, *Nat. Rev. Mol. Cell Biol.*, 2007, **8**, 839–845.
31 T. H. Chun, K. B. Hotary, F. Sabeh, A. R. Saltiel, E. D. Allen and S. J. Weiss, *Cell*, 2006, **125**, 577–591.
32 L. G. Griffith and M. A. Swartz, *Nat. Rev. Mol. Cell Biol.*, 2006, **7**, 211–224.
33 F. Cappiello, B. Casciaro and M. L. Mangoni, *J. Visualized Exp.*, 2018, **133**, 56825.
34 W. G. Payne, D. K. Naidu, C. K. Wheeler, D. Barkoe, M. Mentis, R. E. Salas, D. J. Smith Jr. and M. C. Robson, *Eplasty*, 2008, **8**, 68–90.
35 J. C. Yarrow, Z. E. Perlman, N. J. Westwood and T. J. Mitchison, *BMC Biotechnol.*, 2004, **4**, 21.
36 S. Gu, P. Yu, J. Hu, Y. Liu, Z. Li, Y. Qian, Y. Wang, Y. Gou and F. Yang, *Eur. J. Med. Chem.*, 2019, **164**, 654–664.
37 N. Kramer, A. Walzl, C. Unger, M. Rosner, G. Krupitza, M. Hengstschläger and H. Dolznig, *Mutat. Res.*, 2013, **752**, 10–24.
38 J. A. Caruso, M. T. Duong, J. P. Carey, K. K. Hunt and K. Keyomarsi, *Cancer Res.*, 2018, **78**, 5481–5491.
39 Z. Wang, S. Peng, N. Jiang, A. Wang, S. Liu, H. Xie, L. Guo, Q. Cai and Y. Niu, *Oncotarget*, 2017, **8**, 102361–102370.
40 J. Deng, P. Yu, Z. Zhang, J. Wang, J. Cai, N. Wu, H. Sun, H. Liang and F. Yang, *Eur. J. Med. Chem.*, 2018, **158**, 442–452.
41 R. Gerl and D. L. Vaux, *Carcinogenesis*, 2005, **26**, 263–270.
42 L. H. Aung, R. Li, B. S. Prabhakar, A. V. Maker and P. Li, *Oncotarget*, 2017, **8**, 56582–56579.
43 S. Xiong, T. Mu, G. Wang and X. Jiang, *Protein Cell*, 2014, **5**, 737–749.
44 D. L. Vaux, S. Cory and J. M. Adams, *Nature*, 1988, **335**, 440–442.
45 J. M. Hardwick and L. Soane, *Cold Spring Harbor Perspect. Biol.*, 2013, **5**, a008722.
46 C. Pop, J. Timmer, S. Sperandio and G. S. Salvesen, *Mol. Cell*, 2006, **22**, 269–275.
47 S. H. Park and C. Blackstone, *EMBO Rep.*, 2010, **11**, 515–521.
48 B. Luo and A. S. Lee, *Oncogene*, 2013, **32**, 805–818.
49 G. E. Stutzmann and M. P. Mattson, *Pharmacol. Rev.*, 2011, **63**, 700–727.
50 J. M. Timmins, L. Ozcan, T. A. Seimon, G. Li, C. Malagelada, J. Backs, T. Backs, R. Bassel-Duby, E. N. Olson and M. E. Anderson, *J. Clin. Invest.*, 2009, **119**, 2925–2941.
51 S. J. Marciniak and D. Ron, *Physiol. Rev.*, 2006, **86**, 1133–1149.
52 K. Homma, K. Katagiri, H. Nishitoh and H. Ichijo, *Expert Opin. Ther. Targets*, 2009, **13**, 653–664.
53 I. Kim, W. Xu and J. C. Reed, *Nat. Rev. Drug Discovery*, 2008, **7**, 10131030.
54 S. Oyadomari and M. Mori, *Cell Death Differ.*, 2004, **11**, 381–389.
55 H. P. Harding, Y. Zhang, A. Bertolotti, H. Zeng and D. Ron, *Mol. Cell*, 2000, **5**, 897–904.
56 M. P. Murphy, *Biochem. J.*, 2008, **417**, 1–13.
57 H. U. Simon, A. Haj-Yehia and F. Levi-Schaffer, *Apoptosis*, 2000, **5**, 415–418.
58 K. J. Wu, C. Grandori, M. Amacker, N. Simon-Vermot, A. Polack, J. Lingner and R. Dalla-Favera, *Nat. Genet.*, 1999, **21**, 220–224.
59 Y. Zhao, D. Cheng, S. Wang and J. Zhu, *Nucleic Acids Res.*, 2014, **42**, 10385–10398.
60 X. Wang, P. Zhou, X. Sun, J. Zheng, G. Wei, L. Zhang, H. Wang, J. Yao, S. Lu and P. Jia, *Oncol. Rep.*, 2015, **33**, 3038–3044.
61 B. J. Chen, Y. L. Wu, Y. Tanaka and W. Zhang, *Int. J. Biol. Sci.*, 2014, **10**, 1084–1096.
62 A. Bonni, A. Brunet, A. E. West, S. R. Datta, M. A. Takasu and M. E. Greenberg, *Science*, 1999, **286**, 1358–1362.
63 A. S. Dhillon, S. Hagan, O. Rath and W. Kolch, *Oncogene*, 2007, **26**, 3279–3290.
64 J. Segalés, E. Perdiguero and P. Muñoz-Cánoves, *Front. Cell Dev. Biol.*, 2016, **4**, 91.
65 R. J. Orton, O. E. Sturm, V. Vyshemirsky, M. Calder, D. R. Gilbert and W. Kolch, *Biochem. J.*, 2005, **392**, 249–261.
66 J. Han, J. D. Lee, L. Bibbs and R. J. Ulevitch, *Science*, 1994, **265**, 808–811.

Published on 02 November 2020. Downloaded by Carleton University on 11/21/2020 11:15:23 PM.

67 Y. T. Ip and R. J. Davis, *Curr. Opin. Cell Biol.*, 1998, **10**, 205–219.
68 Y. Sun, X. Yu, M. Li and J. Liu, *Chemosphere*, 2018, **200**, 594–602.
69 G. Pearson, F. Robinson, T. Beers Gibson, B. E. Xu, M. Karandikar, K. Berman and M. H. Cobb, *Endocr. Rev.*, 2001, **22**, 153–183.
70 R. A. Hilger, M. E. Scheulen and D. Strumberg, *Onkologie*, 2002, **25**, 511–518.
71 J. S. Sebolt-Leopold, *Clin. Cancer Res.*, 2008, **14**, 3651–3656.
72 I. Tanida, T. Ueno and E. Kominami, *Methods Mol. Biol.*, 2008, **445**, 77–88.
73 M. Komatsu and Y. Ichimura, *FEBS Lett.*, 2010, **584**, 1374–1378.
74 R. Kang, H. J. Zeh, M. T. Lotze and D. Tang, *Cell Death Differ.*, 2011, **18**, 571–580.
75 S. Abram, C. Maichle-Mössmer and U. Abram, *Polyhedron*, 1998, **17**, 131–143.
76 R. L. Arrowsmith, P. A. Waghorn, M. W. Jones, A. Bauman, S. K. Brayshaw, Z. Hu, G. Kociok-Köhn, T. L. Mindt, R. M. Tyrrell and S. W. Botchway, *Dalton Trans.*, 2011, **40**, 6238–6252.
77 Y. X. Tai, Y. M. Ji, Y. L. Lu, M. X. Li, Y. Y. Wu and Q. X. Han, *Synth. Met.*, 2016, **219**, 109–114.


This journal is © The Royal Society of Chemistry 2020